Neural, Parallel, and Scientific Computations 25 (2017) 345-357

A TWO PATHWAYS MODEL FOR CHEMOTACTIC SIGNALING IN AZOSPIRILLUM BRASILENSE

MUSTAFA ELMAS[1], TANMOY MUKHERJEE[2], VASILIOS ALEXIADES[1], AND GLADYS ALEXANDRE[2]

[1]Mathematics, University of Tennessee, Knoxville, TN 37996, USA
[2]Biochemistry, Cellular and Molecular Biology, University of Tennessee, Knoxville, TN 37996, USA

ABSTRACT. Chemotaxis is a mechanism by which bacteria efficiently and rapidly respond to changes in the chemical composition of their environment, moving towards chemically favorable environments and away from unfavorable ones. The regulation of chemotaxis in bacteria is achieved by a network of interaction proteins constituting a chemotaxis signal transduction pathway. It has been found recently that most motile bacteria have two or more (Che) systems, whereas the model organism Escherichia coli possesses a single chemotaxis system. We present a novel mathematical model that can be used to understand the properties of biological signaling pathways in Azospirillum brasilense. The main implication of our study is that A. brasilense cells utilize two chemotaxis signaling pathways with unequal protein and receptor concentrations.

AMS (MOS) Subject Classification. 92C17, 35L50, 35K57.

1. Introduction

Many organisms live in ever-changing environments and utilize some information processing systems to constantly monitor their surrounding environments for important changes. The ability of organisms to detect and respond to environmental changes is crucial for their metabolism, growth and survival. The process by which bacteria sense changes in their chemical environment and then move towards more favorable and away from toxic environments is known as **chemotaxis** ([9], [13]). In flagellated bacteria, such as Escherichia coli (E. coli), this behavior is achieved by integration signals received from the environment and modulating the rotational direction of their flagella accordingly ([5], [7],[18]). When flagellar motors rotate counterclockwise (CCW), the flagella come together and form a bundle that pushes the cell forward, called *runs*. On the other hand, when one or more of the flagellar motors rotate clockwise (CW), the flagella bundle flies apart and leads to tumbling, changing the swimming direction ([22]). Chemotaxis systems integrate environmental cues into a behavioral

Received June 1, 2017

response by using dedicated signal transduction pathways ([35], [42]). Such a pathway acts as a computational unit: each component of the pathway receives one or more inputs, processes the signals and then generates one or more outputs ([25]). The main output of the chemotaxis signal transduction pathway is phosphorylation of the diffusible signaling protein CheY (Y_p), which decides the CW bias of the cell, i.e., fraction of time the cell spends in tumbling ([44]).

The molecular mechanism of chemotaxis signal transduction has been extensively studied and deciphered in most detail for the model organism E. coli, which possesses a single chemotaxis system ([8], [15]). The chemotaxis pathway in this bacterium is a simple network of protein interactions, pictured in Figure 1. The major players in the pathway are chemoreceptors (MCPs) and cytosolic proteins (Che) ([43]). MCPs, CheW, CheA and CheY constituting an excitation pathway, whereas CheR, CheB and CheZ constitute an adaptation pathway ([41]).

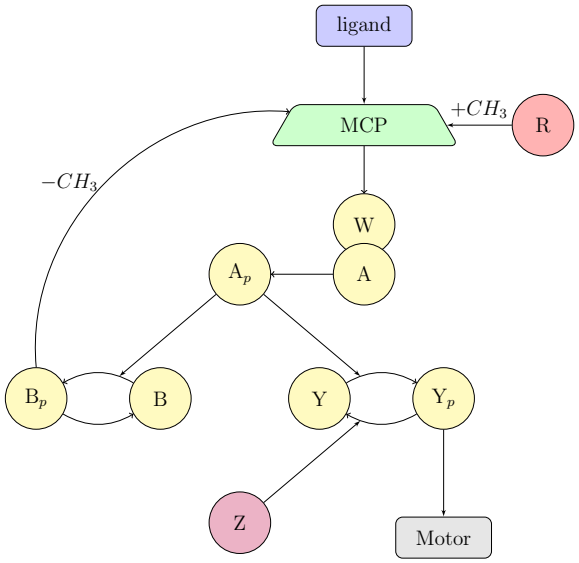

Figure 1. The Chemotaxis Pathway in E. coli.

Bacterial transmembrane receptors (MCPs) possess an extracellular ligand-binding domain crossing the cell membrane to detect chemical stimuli in the environment. The signaling activity of receptors is thought to exist in two states, active (activating CheA autophosphorylation) or inactive (inhibiting CheA autophosphorylation) ([39]). The activity of CheA autophosphorylation is affected by occupancy of receptors. Ligand binding to a chemoreceptor induces a conformational change in receptor proteins and this in turn causes a change in the rate of CheA autophosphorylation. Repellent binding to chemoreceptors increases the autophosphorylation rate of CheA. ([17]). The activated CheA acquires a phosphate group through autophosphorylation. The phosphorylated CheA (A_p), then transfers the phosphate group to the response regulator proteins CheY and CheB. When Y_p binds to FliM, a component of the motor switch complex, it promotes a switch in the rotational direction from CCW

to CW, which in turn results a change in the swimming direction of the motile cell. Signal termination is crucial for the bacterial cells to continuously sense and appropriately respond to environmental stimuli. Even though Y_p is dephosphorylated spontaneously, this process is enhanced by the phosphatase CheZ ([14]). This is the excitation phase of the bacterial chemotaxis pathway.

Cells return to prestimulus steady state behavior in the presence of the stimulus after an initial response to changes in environmental cues. This adaptation mechanism is an essential component of bacterial chemotaxis system since it allows the system to compansate for the presence of continued stimulation, and to be ready to respond to futher stimuli ([3]). The adaptation phase of chemotaxis system involves the methyltransferase CheR and the methylesterase CheB. CheR adds methyl groups to chemotaxis receptors whereas phosphorylated CheB (B_p), removes the methyl groups. CheR preferentially methylates receptors in an inactive conformation, thus the ability to activate CheA autophosphorylation is increased, which in turn leads to elevated Y_p concentration and tumbling. B_p preferentially demethylates receptors in an active conformation, thus the ability of receptors to activate CheA autophosphorylation is reduced, which in turn leads to decreased Y_p concentration and less tumbling ([26], [30]). The demethylation process serves as the feedback control of the chemotaxis system ([4]).

2. **Chemotaxis Pathway in A. Brasilense**

It has been found recently that many bacteria possess chemotaxis pathways that are more complicated than the well-known example of E. coli. They contain multiple homologues of the proteins found in E. coli pathway ([37]); may contain chemotaxis proteins not found in E.coli: CheC, CheD and CheV ([30]); may not contain some of the E. coli proteins: CheR and CheB ([40]). Furthermore, some bacteria such as Azospirilum brasilense, Rhodobacter sphaeroides, Rhodospirillum centenum and Myxococcus xanthus possess multiple homologues of the E. coli chemotaxis system ([32], [19], [16]).

A. brasilense is a motile soil alphaproteobacterium that colonizes the rhizosphere of various agronomically important grasses and cereals, promoting plant growth. These gram-negative bacteria have the ability to fix atmospheric nitrogen under low oxygen concentration (microaerophilic conditions) ([2]). A. brasilense cells swim by rotating a single bidirectional polar flagellum ([23]). The available genome sequence of A. brasilense indicates the presence of four distinct chemotaxis operons Che1, Che2, Che3, and Che4. Experimental evidence indicates that signals from Che1 and Che4 are integrated during chemotaxis to produce an appropriate response to physicochemical cues ([34], [6], [20], [27]).

The signal transduction proteins are organized and localized into two distinct sensory clusters and the signaling output of both clusters are required for chemotaxis and aerotaxis in A. brasilense. The connectivity of signaling pathways in A. brasilense is unknown. Mathematical modeling has provided considerable insight into the mechanism of chemotactic signaling in E. coli and other bacteria ([25], [24], [31], [38], [19]). To understand the role of each signaling cluster, we present a mathematical model of the simplest chemotaxis network in A. brasilense, pictured in Figure 2, based on experimental observations. The model enables us to make testable predictions of the system behavior under different experimental conditions, which leads to new information that has not been uncovered by experiments or is unattainable (or very difficult to attain) experimentally.

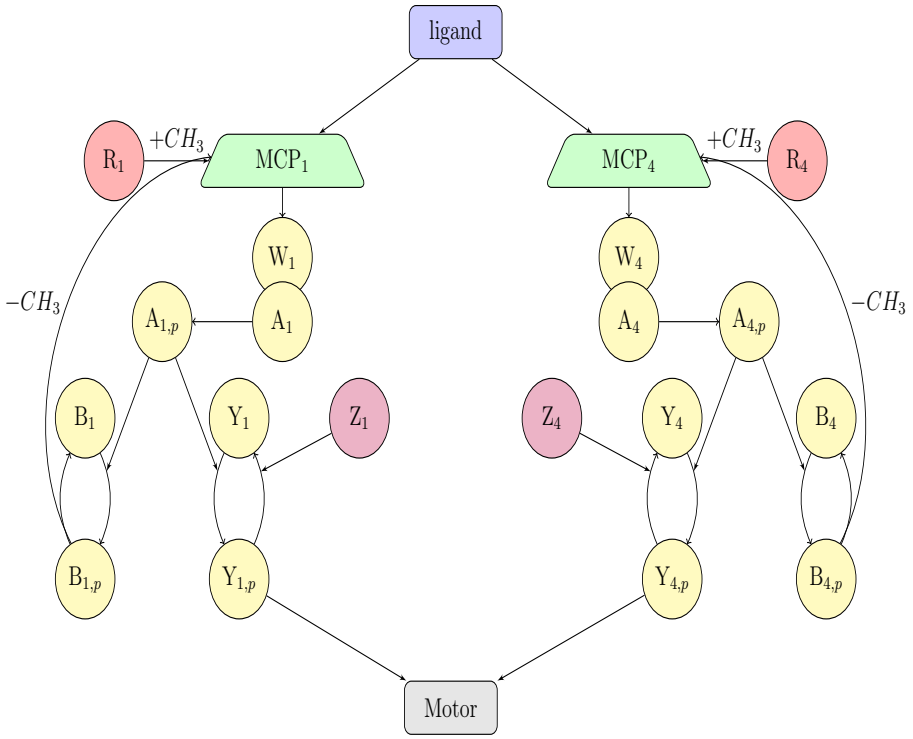

Figure 2. Chemotaxis Pathways in A. brasilense. The currently known localization and connectivity of the chemotaxis pathway in A. brasilense is shown. Active MCP_1 [MCP_4] increases autophosphorylation of $CheA_1$ [$CheA_4$], then phosphoryl groups are transferred from $CheA_1$ [$CheA_4$] to $CheY_1$ [$CheY_4$] and $CheB_1$ [$CheB_4$]. While phoshorylated $CheY_1$ ($Y_{1,p}$), [$CheY_4$ ($Y_{4,p}$)] hydrolysis is enhanced by the phosphatase $CheZ_1$ [$CheZ_4$], phoshorylated $CheB_1$ ($B_{1,p}$) [$CheB_4$ ($B_{4,p}$)] dephosphorylates spontaneously. Total phosphorylated CheY (sum of $Y_{1,p}$ and $Y_{4,p}$) interacts with motor FliM protein of the flagella to increase CW bias of the flagella motor.

3. MODEL

From detection of physicochemical cues to the activation of the flagellar motor, a series of chemical reactions are involved in relaying and regulating the signal. These reactions are split into three modules: sensing, signal transduction, and actuation, listed in Table 1. Assuming mass-action kinetics, these reactions can be modeled mathematically by ordinary differential equations (ODEs), which are described below.

Ligand binding	$T_{n,mv} + L \leftrightarrow T_{n,m}L \ (\equiv T_{n,mo})$	
Methylation	$T_{n,m} + R_n \leftrightarrow T_{n,m}R_n$	$T_{n,m}R_n \rightarrow T_{n,m+1} + R_n$
Demethylation	$T_{n,m} + B_{n,p} \leftrightarrow T_{n,m}B_{n,p}$	$T_{n,m}B_{n,p} \rightarrow T_{n,m-1} + B_{n,p}$
Phosphorylation	$T_n^a + A_{n,u} \rightarrow A_{n,p}$	
	$A_{n,p} + Y_{n,u} \rightarrow A_{n,u} + Y_{n,p}$	
	$A_{n,p} + B_{n,u} \rightarrow A_{n,u} + B_{n,p}$	
Dephosphorylation	$Y_{n,p} + Z_n \rightarrow Y_{n,u}$	
	$B_{n,p} \rightarrow B_{n,u}$	
Motion of cell	$Y_{p,tot} + FliM \rightarrow CW$	

Table 1. Reactions in the signal transduction pathways

Since both signal transduction pathways act in the same fashion, we describe the ligand-binding/unbinding of the receptors, methylation/demethylation of the receptors and the signal transduction of the signals for one generic pathway, called n^{th} pathway where $n = 1$ indicates the receptor and proteins belonging to the first pathway, while $n = 4$ indicates the second pathway.

We use the label $T_{n,m\lambda}$ for chemotaxis receptors, where m indicates methylation level (the number of methyl group added to the receptor, $m = 0, 1, 2, 3, 4$) and λ represents the status of the receptor whether ligand bound (o, for occupied) or ligand unbound (v, for vacant). Subscripts are used to describe whether the cytosolic protein is phosphorylated (p) or unphosphorylated (u), and (tot) is used to label total concentrations of different proteins. Superscript (i) indicates the receptor is in inactive form, superscript (a) indicates the receptor is in active form, thus able to phosphorylate CheA.

3.1. Sensing.

Since the timescale for ligand (L) binding is much shorter than the methylation and phosphorylation timescales, the ligand binding and unbinding can be assumed in quasi-equilibrium and the ligand bound and unbound receptor concentrations for $T_{n,m}$ in each methylation level m are given respectively by,

$$T_{n,mo} = \frac{L}{K_{n,d} + L} T_{n,m}, \qquad m = 0, 1, 2, 3, 4, \tag{3.1}$$

$$T_{n,mv} = \frac{K_{n,d}}{K_{n,d} + L} T_{n,m}, \qquad m = 0, 1, 2, 3, 4, \tag{3.2}$$

where $K_{n,d}$ is the receptor-ligand dissociation constants for $T_{n,m}$. The total receptor concentration for these receptors at methylation level m is given by,

$$T_{n,m} = T_{n,mv} + T_{n,mo}. \tag{3.3}$$

The total receptor concentration for T_n is given by,

$$T_{n,tot} = \sum_{m=0}^{4} T_{n,m}. \tag{3.4}$$

The total concentration of active receptors $T_{n,m}$ is given by,

$$T_n^a = \sum_{m=0}^{4} P_{n,m}(L) T_{n,m}, \tag{3.5}$$

while the total concentration of inactive receptors $T_{n,m}$ is given by,

$$T_n^i = \sum_{m=0}^{4} (1 - P_{n,m}(L)) T_{n,m}, \tag{3.6}$$

where $P_{n,m}(L)$ denotes the total probability of the receptor complex being in active state for $T_{n,m}$ and it is the sum of the probabilities of the ligand bound ($P_{n,mo}$) and non ligand bound ($P_{n,mv}$) being in active state and are given by,

$$P_{n,m}(L) = P_{n,mo}(L) \frac{L}{K_{n,d} + L} + P_{n,mv}(L) \frac{K_{n,d}}{K_{n,d} + L}. \tag{3.7}$$

The model assumes that $CheR_n$ (R_n) binds to the inactive receptors (T_n^i) and phosphorylated $CheB_n$ ($B_{n,p}$) binds to active receptors (T_n^a) ([26], [24]). Assuming that the methylation and demethylation reactions follow Michaelis-Menten kinetics, the rate is given respectively by,

$$r_{n,B} = k_{n,b} \frac{B_{n,p}}{K_{n,B} + T_n^a}, \tag{3.8}$$

$$r_{n,R} = k_{n,r} \frac{R_n}{K_{n,R} + T_n^i}, \tag{3.9}$$

where $k_{n,b}$ and $k_{n,r}$ are catalytic constants and $K_{n,B}$ and $K_{n,R}$ are Michaelis constants for the receptors methylation and demethylation reactions, respectively.

The rate of methylation is proportional to the concentration of inactive receptors $(1 - P_{n,m}(L))T_{n,m}$ and the rate of demethylation is proportional to the concentration of active receptors $P_{n,m}(L)T_{n,m}$.

The kinetic equations of receptor $T_{n,m}$ can be written as,

$$\frac{dT_{n,m}}{dt} = J_{n,m-1} - J_{n,m}, \quad m = 0, 1, 2, 3, 4, \tag{3.10}$$

where $J_{n,m}$ is the net flux from methylation state m to state $m+1$ for the receptors $T_{n,m}$, which is just the difference of methylation and demethylation rates between these two states namely,

$$J_{n,m} = r_{n,R}(1 - P_{n,m}(L))T_{n,m} - r_{n,B}P_{n,m+1}(L)T_{n,m+1}, \qquad m = 0, 1, 2, 3. \tag{3.11}$$

The end conditions for methylation fluxes are zero

$$J_{n,-1} = J_{n,4} = 0.$$

3.2. **Signal Transduction.**

The receptor properties, ligand-bound or ligand-unbound, influence the activity of $CheA_n$ and the active chemotaxis receptors increase the activity of $CheA_n$, denoted by A_n. Once $CheA_n$ is activated, it acquires a phosphate group through autophosphorylation and transfers the phosphate group to $CheY_n$ (Y_n) and $CheB_n$ (B_n). While phoshorylated $CheY_n$ ($Y_{n,p}$), hydrolysis is enhanced by the phosphatase $CheZ_n$, phoshorylated $CheB_n$ ($B_{n,p}$) dephosphorylates spontaneously. Total phosphorylated CheY (sum of $Y_{n,p}$) interacts with FliM protein of the flagella to increase CW bias of the flagella motor. The kinetic equations for signal transduction are given below:

$$\frac{dA_{n,p}}{dt} = a_{i,P}T_n^a A_{n,u} - a_{n,Y}A_{n,p}Y_{n,u} - a_{n,B}A_{n,p}B_{n,u} \tag{3.12}$$

$$\frac{dY_{n,p}}{dt} = a_{n,Y}A_{n,p}Y_{n,u} - d_{n,Z}Y_{n,p} \tag{3.13}$$

$$\frac{dB_{n,p}}{dt} = a_{n,B}A_{n,p}B_{n,u} - d_{n,B}B_{n,p} \tag{3.14}$$

where $A_{n,u} = A_{n,tot} - A_{n,p}$, $Y_{n,u} = Y_{n,tot} - Y_{n,p}$ and $B_{n,u} = B_{n,tot} - B_{n,p}$. Here $a_{n,P}$ is the phosphorylation rate of A_n by T_n^a active receptors. $a_{n,Y}$ and $a_{n,B}$ are phosphorylation transfer rate from A_n to Y_n and B_n. Finally, $d_{n,Z}$ and $d_{n,B}$ are dephosphorylation rate of $Y_{n,p}$ by Z_n and spontaneous dephosphorylation rate of $B_{n,p}$, respectively.

3.3. **Motor actuation.**

The above intracellular signaling pathway determines the concentration of phosphorylated CheY (Y_p), which in turn binds to the flagellar motor (FliM) and decides the CW bias of the cell, i.e., the fraction of time the cell spends in tumbling ([40]). Using a Hill function with an appropriate Hill coefficient (h) to relate CW bias and phosphorylated CheY ([10], [44]), we can quantify this as

$$Y_p = Y_{1,p} + Y_{4,p}, \tag{3.15}$$

$$CW = \frac{(Y_p)^h}{(H_S)^h + (Y_p)^h}, \tag{3.16}$$

where H_S is a half saturation constant.

4. SIMULATIONS

As we lack protein concentrations and kinetic parameters for A. brasilense, we use the concentrations and parameters from the E. coli literature, listed in Table 2. The main output of the models, described in Figure 1 and Figure 2, is phosphorylated CheY (Y_p). Relaxation time of Y_p is calculated as the width of Y_p(t) curve at 20% of its amplitude, as shown in Figure 3.

Parameter	Description	Value	Units	Source
$T_{1,tot}$	T_1 concentration	7.5	μM	[21]
$T_{4,tot}$	T_4 concentration	2.5	μM	[24]
$A_{1,tot}$	$CheA_1$ concentration	2.5	μM	[24]
$A_{4,tot}$	$CheA_4$ concentration	7.5	μM	[21]
$B_{1,tot}$	$CheB_1$ concentration	0.542	μM	[24]
$B_{4,tot}$	$CheB_4$ concentration	1.626	μM	[24]
$Y_{1,tot}$	$CheY_1$ concentration	9.0	μM	[33]
$Y_{4,tot}$	$CheY_4$ concentration	27.0	μM	[33]
$R_{1,tot}$	$CheR_1$ concentration	0.080	μM	[21]
$R_{4,tot}$	$CheR_4$ concentration	0.240	μM	[21]
$a_{1,p}$	$CheA_1$ autophosphorylation by T_1	15.5	s^{-1}	[35]
$a_{4,p}$	$CheA_4$ autophosphorylation by T_4	15.5	s^{-1}	[35]
$a_{1,Y}$	$CheA_1 \to CheY_1$ phosphorus transfer rate	100	$\mu M^{-1}s^{-1}$	[36]
$a_{4,Y}$	$CheA_4 \to CheY_4$ phosphorus transfer rate	100	$\mu M^{-1}s^{-1}$	[36]
$a_{1,B}$	$CheA_1 \to CheB_1$ phosphorus transfer rate	30	$\mu M^{-1}s^{-1}$	[36]
$a_{4,B}$	$CheA_4 \to CheB_4$ phosphorus transfer rate	30	$\mu M^{-1}s^{-1}$	[36]
$d_{1,B}$	$CheB_1$ dephosphorylation rate	1	s^{-1}	[26]
$d_{4,B}$	$CheB_4$ dephosphorylation rate	1	s^{-1}	[26]
$d_{1,Z}$	$CheY_1$ dephosphorylation rate	30	s^{-1}	[33]
$d_{4,Z}$	$CheY_4$ dephosphorylation rate	30	s^{-1}	[33]
$k_{1,B}$	$CheB_1$ catalytic constant	0.155	s^{-1}	[25]
$k_{4,B}$	$CheB_4$ catalytic constant	0.155	s^{-1}	[25]
$k_{1,R}$	$CheR_1$ catalytic constant	0.255	s^{-1}	[25]
$k_{4,R}$	$CheR_4$ catalytic constant	0.255	s^{-1}	[25]
$K_{1,B}$	$CheB_1$ Michaelis constant	0.540	μM	[12]
$K_{4,B}$	$CheB_4$ Michaelis constant	0.540	μM	[12]
$K_{1,R}$	$CheR_1$ Michaelis constant	0.364	μM	[12]
$K_{4,R}$	$CheR_4$ Michaelis constant	0.364	μM	[12]
$K_{1,d}$	The receptor-ligand dissociation rate for T_1	250	μM	[31]
$K_{4,d}$	The receptor-ligand dissociation rate for T_4	250	μM	[31]
H_S	Half saturation constant of $CheY_p$	3.1	μM	[10]
h	Hill coeeficient	5.5		[10]
		m 0 1 2 3 4		
$P_{n,m\lambda}$	Relative activity of $T_{n,m}$	v 0 0.65 0.75 0.95 1.0		[24]
		o 0 0.0 0.01 0.05 1.0		

Table 2. Parameters of the chemotaxis pathways in A. brasilense.

4.1. Relaxation time of Y_p in E. coli.

Figure 3(A) shows Y_p history of E. coli model of Figure 1. Relaxation time is 87 seconds.

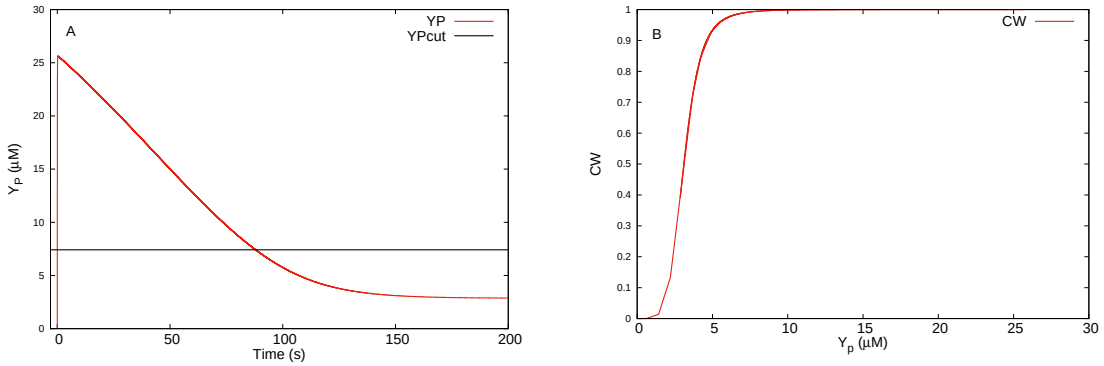

Figure 3. **(A)** Evolution of Y_p in E. coli. Relaxation time of Y_p is 87 seconds. **(B)** Characteristic response of flagellar motor as a function of Y_p

4.2. **Relaxation time of Y_p in A. brasilense.**

For the two pathways model of Figure 2 we examine two cases, one with equal concentrations in the two pathways and another with unequal.

4.2.1. *Case I: equal concentrations in the two pathways.*

Taking the concentrations of proteins and receptors in Che1 and Che4 pathways to be the same, with values as in Table 2, Figure 4(A) shows the history of phosphorylated CheY (Y_p). Relaxation time is 121 seconds.Thus, the two-pathways model produces longer Relaxation time than the one produced in §4.1, which agrees with experimental results.

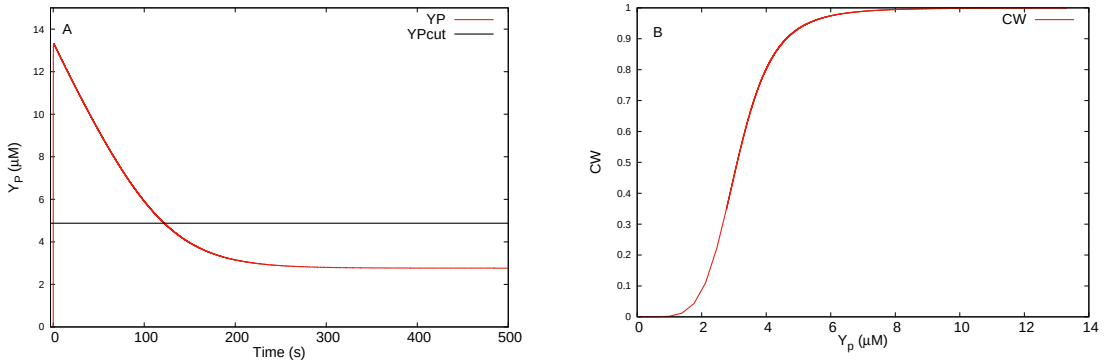

Figure 4. **(A)** Evolution of Y_p in A. brasilense with equal concentrations in both pathways. Relaxation time of Y_p is 121 seconds. **(B)** Characteristic response of flagellar motor as a function of Y_p

4.2.2. *Case II: unequal concentrations in the two pathways.*
Now we take oncentrations of the proteins in Che4 pathway to be 3 times higher than the ones in Che1 pathway, while receptor concentrations in Che1 pathway to be 3 times higher than the ones in Che4 pathway, as found in experiments ([1], [20], [27]). Figure 5A shows the evolution of phosphorylated CheY. As it can be seen from the Y_p concentration profile and its relaxation time, which is 248 seconds, the two-pathways model, with more abundant proteins concentrations in Che4 pathway, produces longer relaxation time than the one in §4.2.1, in agreement with experimental results.

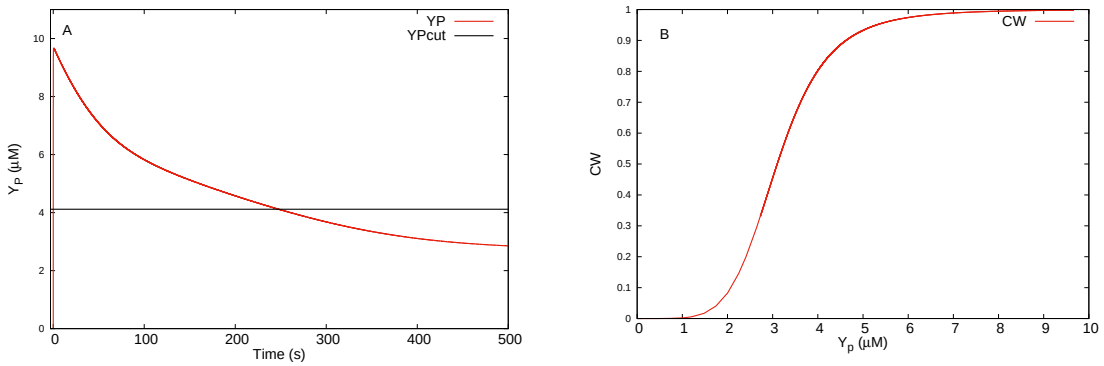

Figure 5. (A) Evolution of Y_p in A. brasilense with higher protein concentrations in Che4 pathway. Relaxation time of Y_p is 248 seconds. **(B)** Characteristic response of flagellar motor as a function of Y_p

5. DISCUSSION

It has been found that most motile bacteria possess multiple chemotaxis systems, in contrast to the model organism E. coli, which possesses one chemotaxis system ([41], [28]). The available genome squence of of A. brasilense indicates the presence of four distinct chemotaxis operons with multiple homologues of the proteins found in E. coli ([11]). A. brasilense cells use two chemotaxis systems to regulate chemotaxis. The molecular mechanism by which A. brasilense bacteria use to execute chemotaxis is different from that in E. coli. On the other hand, there are many similarities with chemotaxis in Rhodobacter sphaeroides, a bacterial species that has been extensively studied as a model organism for organisms for multiple chemotaxis pathways ([29]). R. sphaeroides bacteria use two chemotaxis systems, named Che2 and Che3, to regulate the rotation of flagellar motor ([19]).

Experimental evidence shows that signaling outputs from Che1 and Che4 pathways, likely mediated via $CheY_1$ and $CheY_4$ are integrated at flagellar motor level in order to produce an appropriate response to changes in environmental conditions ([27]). The concentration of proteins in Che4 operon are more abundant, about 3

times, than the concentration of proteins in Che1 operons, while the concentration of receptors in Che1 operon is about 3 times higher than those in Che4 operon ([1], [20], [27]). Higher abundance of proteins in Che4 pathway will produce higher relaxation time after the cells are challenged with an attractant (or a repellent) via increasing (or decreasing) ligand concentration in experiments ([20]). We developed a mathematical model of simplest chemotaxis pathways based on these experimental results. The implication of our study is that A. brasilense cells use at least two chemotaxis system to regulate relaxation time in response to changes in the environment they live in. The numerical results in section 4 agree well with experimental results, at least qualitatively.

Unfortunately, using a more realistic model to simulate chemotaxis pathways in A. brasilense is still limited by the lack of quantitative experimental data and kinetic studies. For example, the contribution of other Che systems, Che2 and Che3, and other proteins in the A. brasilense genome to chemotaxis, cross-talk and synchronization of the two sensory pathways, the mechanism of integrating the signals produced by each of the signaling pathways to control the flagellar response, are yet unclear and under study.

ACKNOWLEDGMENTS

Partially supported by NSF Grant R01-1052148.

REFERENCES

[1] Aksenova. A, *Localization of chemoreceptors in Azospirillum brasilense. Masters Thesis*, University of Tennessee, 2014.

[2] G. Alexandre, *More than one way to sense chemicals*, *Bacteriology*, 183:4681-4686, 2001.

[3] U. Alon, M.G. Surette, N. Barkai and S. Leibler, *Robustness in bacteria chemotaxis*, *Nature*, 397:168–171, 1999.

[4] N. Barkai and S. Leibler, *Robustness in simple biochemical networks*, *Nature*, 387:913–917, 1997.

[5] H. C. Berg and D. A. Brown, *Chemotaxis in Escherichia coli analysed by three-dimensional tracking*, *Nature*, 239:500504, 1972.

[6] A. N. Bible, B. B. Stephens, D. R. Ortega, Z. Xie and G. Alexandre, *Function of a chemotaxis-like signal transduction pathway in modulating motility, cell clumping, and cell length in the alphaproteobacterium Azospirillum brasilense*, *Journal of Bacteriology*, 190:636575, 2008.

[7] K. A. Borkovich and M. I. Simon,*The dynamics of protein phosphorylation in bacterial chemotaxis*, *Cell*, 63: 13391348, 1990.

[8] D. Bray, R. B. Bourret, and M. I. Simon, *Computer simulation of the phosphorylation cascade controlling bacterial chemotaxis*, *Mol. Biol. Cell.*, 4:469482, 1993.

[9] A. Bren, and M. Eisenbach, *How signals are heard during bacterial chemotaxis: protein-protein interactions in sensory signal propagation*, *J. Bacteriol.* 182:68656873, 2000.

[10] P. Cluzel, M.G. Surette and S. Leibler, *An ultrasensitive bacterial motor revealed by monitoring signaling proteins in single cells*, *Science*, 287:1652–1655, 2000.

[11] F. Wisniewski-Dye, K. Borziak, G. Khalsa-Moyers, G.Alexandre,L. O. Sukharnikov, K. Wuichet and I. B. Zhulin, *Azospirillum genomes reveal transition of bacteria from aquatic to terrestrial environments*, *PLoS Genetics*, 7:e1002430, 2011.

[12] T. Emonent and P. Cluzel, *Relationship between cellular response and behavioral variability in bacterial chemotaxis*, *Proc. Natl. Acad. Sci. USA*, 105:3304-3309, 2008.

[13] M. Eisenbach, *Chemotaxis, chapter 3*, *Imperial College Press* 2004.

[14] M. Eisenbach, *Control of bacterial chemotaxis*, *Molecular Microbiology*, 20:903-910, 1996.

[15] J. J. Falke, R. B. Bass, S. L. Butler, S. A. Chervitz, and N. A. Danielson, *The two-component signaling pathway of bacterial chemotaxis*, *Annu. Rev. Cell Dev. Biol.*, 13:457512, 1997.

[16] S. Fan and R. G. Endres, *A minimal model for metabolism-dependent chemotaxis in Rhobactersphaeroides*, *Interface Focus*,

[17] J. A. Gegner, D. R. Graham, A. F. Roth and F. W. Dahlquist, *Assembly of an MCP receptor, CheW, and kinase CheA complex in the bacterial chemotaxis signal transduction pathway*, *Cell*, 70:975982, 1992.

[18] R. N. Grishanin, D. E. Gauden and J. P. Armitage, *Photoresponses in Rhodobacter sphaeroides: role of photosynthetic electron transport*, *J. Bacteriol.*, 179:2430, 1997.

[19] A. Hamadeh, M. J. Roberts, A. Elias, P. Maini, P. McSharry, E. Patrick, J. P. Armitage and A. Papachritodoulou, *Feedback control architecture and the bacterial chemotaxis network*, *PLOS Computation Biology*, 7:1:15, 2011.

[20] D. Kumar, *Characterization of the Che4 Signal Transduction Pathway in Taxis Behaviors of Azospirillum brasilense. Masters Thesis*, University of Tennessee, 2012.

[21] L. Mingshan and G. L. Hazelbauer, *Cellular Stoichiometry of the Components of the Chemotaxis Signaling Complex*, *Journal of Bacteriology*, 186:3687-3694, 2004.

[22] R. M. Macnab and E. D. Koshland, *The gradient-sensing mechanism in bacterial chemotaxis*, *Proc. Natl. Acad. Sci.*, 69:2509-2512, 1972. 4:1-13, 2014.

[23] B. C. Mazzag, I. B. Zhulin and A. Mogilner, *Model of bacterial band formation in aerotaxis*, *Biophys. J.*, 85:35583574, 2003.

[24] B. A. Mello and Y. Tu, *Perfect and near-perfect adaptation in a model of bacterial chemotaxis*, *Biophysical Journal*, 84:2943–2956, 2003.

[25] C. J. Morton-Firth, T. S. Shimizu, and D. Bray, *A free-energy-based stochastic simulation of the tar receptor complex*, *J. Mol. Biol.* 286:10591074, 1999.

[26] C. J. Morton-Firth, and D. Bray, *Predicting temporal fluctuations in an intracellular signalling pathway*, *J. Theor. Biol.* 192:117128, 1998.

[27] T. Mukherjee, D. Kumar, N. Burriss, Z. Xie, and G. Alexandre, *Azospirillum brasilense chemotaxis depends on two signaling pathways regulating distinct motility parameters*, *Journal of Bacteriology*, 198:1764-1772, 2016.

[28] S. L. Porter, G. H. Wadhams and J. P. Armitage, *Signal processing in complex chemotaxis pathways*, *Narute reviews, Microbiology*, 9:153-165, 2011.

[29] S. L. Porter and J. P. Armitage, *Phosphotransfer in Rhodobacter sphaeroides chemotaxis*, *J. Mol. Biol.*, 324:3545, 2002.

[30] C. V. Rao, G. D. Glekas and G. W. Ordal, *The three adaptation systems of Bacillus subtilis chemotaxis*, *Trends Microbiol.*, 16:480487, 2008.

[31] C. V. Rao, J. R. Kirby, and A. P. Arkin, *Design and diversity in bacterial chemotaxis: a comparative study in Escherichia coli and Bacillus subtilis*, *PLoS Biol.*, 2:e49, 2004.

[32] M. J. Roberts, A. Elias, A. Hamadeh, P. Maini, P. McSharry, E. Patrick, J. P. Armitage and A. Papachritodoulou, *A model invalidation-based approach for elucidating biological signalling pathways, applied to the pathway in R. sphaeroides*, *BMC Systems Biology*, 3:1:14, 2009.

[33] B. E. Scharf, K. A. Fahrner, L. Turner, and H. C. Berg, *Control of direction of flagellar rotation in bacterial chemotaxis*, *Proc. Natl. Acad. Sci. USA.*, 95:201206, 1998.

[34] B. B. Stephens, S. N. Loar and G. Alexandre, *Role of CheB and CheR in the Complex Chemotactic and Aerotactic Pathway of Azospirillum brasilense*, *Journal of Bacteriol.*, 188:4759-4768, 2006.

[35] V. Sourjik, and H. C. Berg, *Receptor sensitivity in bacterial chemotaxis*, *Proc. Natl. Acad. Sci. USA*, 99:123127, 2002.

[36] V. Sourjik, and H. C. Berg, *Binding of the Escherichia coli response regulator CheY to its target measured in vivo by fluorescence resonance energy transfer*, *Proc. Natl. Acad. Sci. USA*, 99:1266912674, 2002.

[37] M. J. Tindall, S. L. Porter, P. K. Maini and J. P. Armitage, *Modeling chemotaxis reveals the role of reversed phosphotransfer and a bi-functional kinase-phosphatase*, *PLoS Comput. Biol.*, 6:e1000896, 2010.

[38] M. J. Tindall, P. K. Maini, S. L. Porter, and J. P. Armitage, *Overview of mathematical approaches used to model bacterial chemotaxis II: bacterial populations*, *Bull. Math. Biol.*, 70:15701607, 2008.

[39] M. J. Tindall, S. L. Porter, P. K. Maini, G. Gaglia and J. P. Armitage, *Overview of mathematical approaches used to model bacterial chemotaxis I: the single cell*, *Bull. Math. Biol.*, 70:15251569, 2008.

[40] G. H. Wadhams and J. P. Armitage, *Making sense of it all: bacterial chemotaxis*, *Nature Rev. Mol. Cell. Biol.*, 5:10241037, 2004.

[41] K. Wuichet and I. B. Zhulin, *Origins and diversification of a complex signal transduction system in prokaryotes*, *Sci. Signal.*, 3:ra50, 2010.

[42] N. Vladimirov and V. Sourjik, *Chemotaxis: how bacteria use memory*, *Biol. Chem.*, 390:1097–1104, 2009.

[43] J. Yuan and H. C. Berg, *Ultrasensitivity of an adaptive bacterial motor*, *J. Mol. Bio*, 425:1760-1764, 2013.

[44] J. Yuan, R. . Branch, B.G. Hosu and H. C. Berg, *Adaptation at the output of the chemotaxis signalling pathway*, *Letter*, 484:233-237, 2012.